Electronic Supplementary Material (ESI) for RSC Advances.

Supplementary Materials

Table of context

11	**Fig. S11.** H_2 bubbles.
12	**Fig. S12.** (a) Dependence of the peak current for the $Cu^{II/I}$ couple at $E_{1/2}$= -0.21 V. (b) Scan rate dependence of precatalytic waves for a 0.10 mM solution of complex **1** in buffer (pH 8.7), at scan rates from 120 to 200 mV/s. (c) Linear fitting plot of i_{cat}/i_d *vs* $v^{-1/2}$ for TOF calculation.
13	**Fig. S13.** (a) Scan rate dependence of precatalytic waves for the $Cu^{IV/III}$ couple at $E_{p,a}$ = 1.20 V in buffer (pH 10.8), at scan rates from 100 to 200 mV/s. (b) Linear fitting plot of i_{cat}/i_d *vs* $v^{-1/2}$ for TOF calculation.
14	**Fig. S14.** O_2 bubbles.
15	**Fig. S15.** Charge buildup of 0.25 M phosphate buffer at pH 10.8.
16	**Fig. S16.** Extended controlled potential electrolysis of 2.8 μM complex **1**, showing charge buildup versus time with an applied potential of -1.40 V *vs* Ag/AgCl Conditions: 0.25 M buffer solution, pH 7, GC working electrode (1.25 cm^2), Pt wire counter electrode, 36 h.
17	**Fig. S17.** Extended controlled potential electrolysis of 4.9 μM complex **1** in 0.25 M phosphate buffer at pH 10.8, showing charge buildup versus time with an applied potential of 1.40 V vs Ag/AgCl. ITO working electrode (1.25 cm^2), Pt counter electrode, 36 h.
18	**Fig. S18.** (a) Cyclic voltammograms of complex **1** (0.10 mM) in 0.25 M phosphate buffer (pH 7.0) at a glassy carbon electrode and a scan rate of 100 mV/s with different concentration for (a) water reduction and (b) water oxidation.
19	**Eq. 2** The calculation of TOF-1
20	**Eq. 3** The calculation of TOF-2

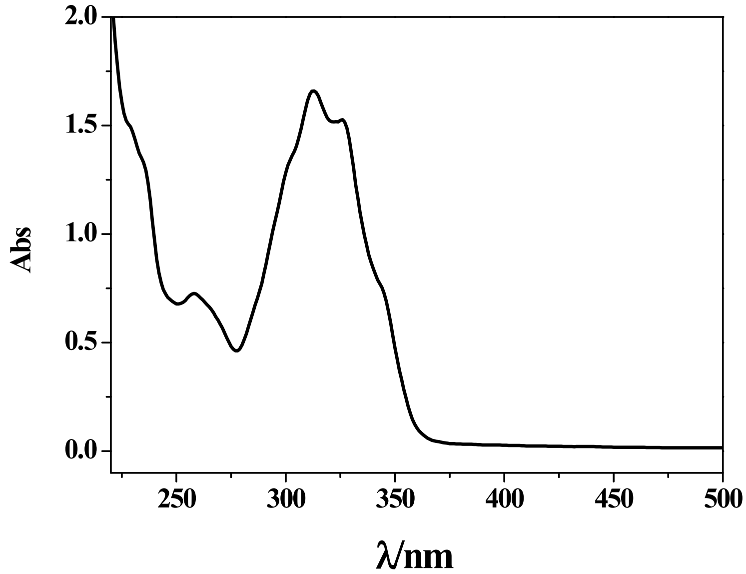

Fig. S1. UV-Vis spectrum of complex **1** in water.

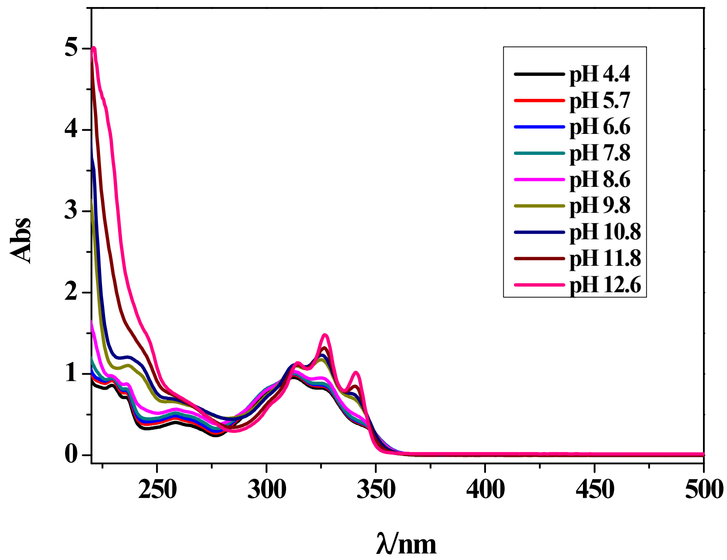

Fig. S2. UV-Vis spectra of complex **1** in buffer solutions at different pH values.

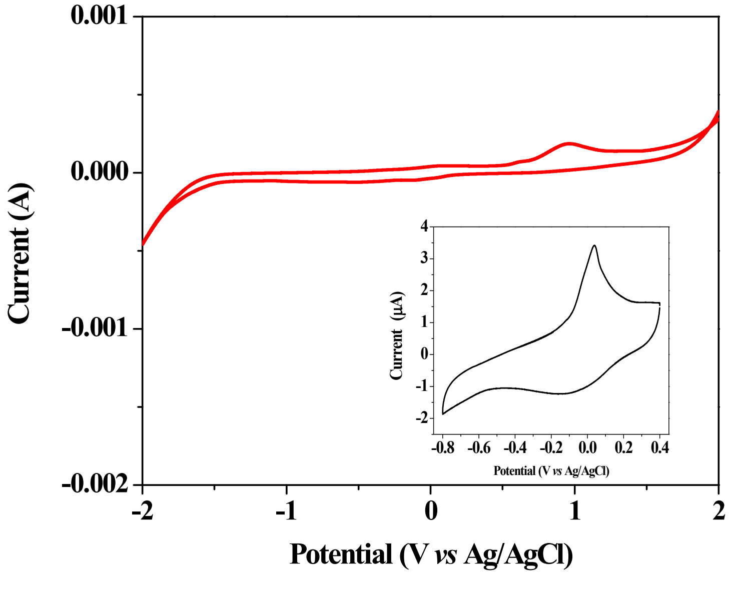

Fig. S3. Cyclic voltammogram of complex **1** (0.1 mM). Conditions: GC working electrode (1 mm diameter), Pt wire counter electrode, Ag/AgCl reference electrode and 100 mV/s. The inset shows a magnified view of the Cu^{II}/Cu^{I} couple.

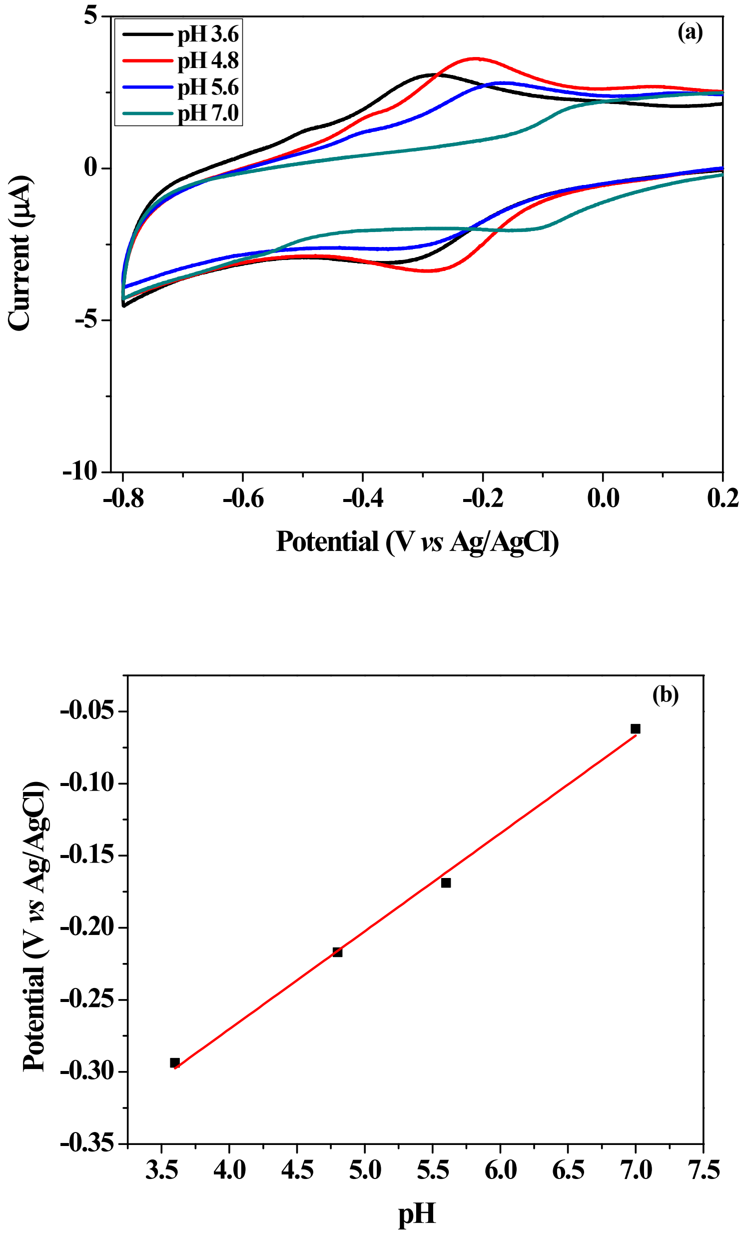

Fig. S4. (a) Cyclic voltammograms of complex **1** (0.1 mM) in different pHs. Conditions: 0.25 M phosphate buffers, scan rate = 100 mV/s, GC working electrode (1 mm diameter), Pt wire counter electrode, Ag/AgCl reference electrode. (b) Pourbaix diagram for the $Cu^{II/I}$ redox couple of complex **1** in aqueous buffer.

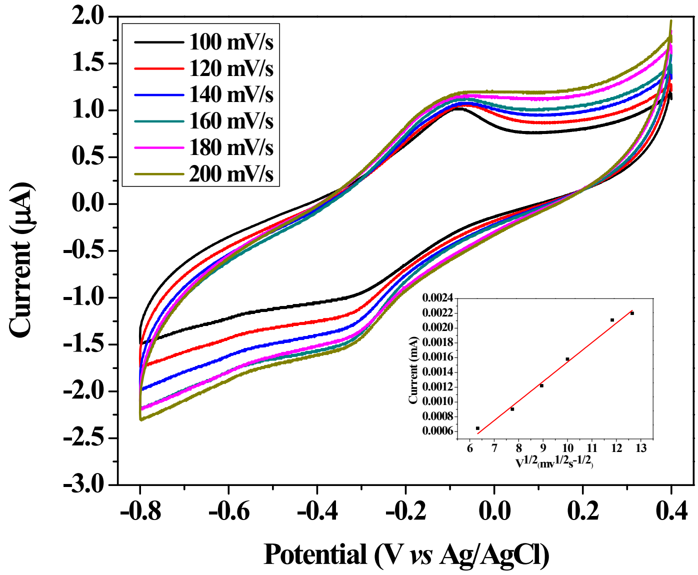

Fig. S5. Scan rate dependence of precatalytic waves for a 0.10 mM solution of complex **1** (0.1 M KNO_3), at scan rates from 100 to 200 mV/s.

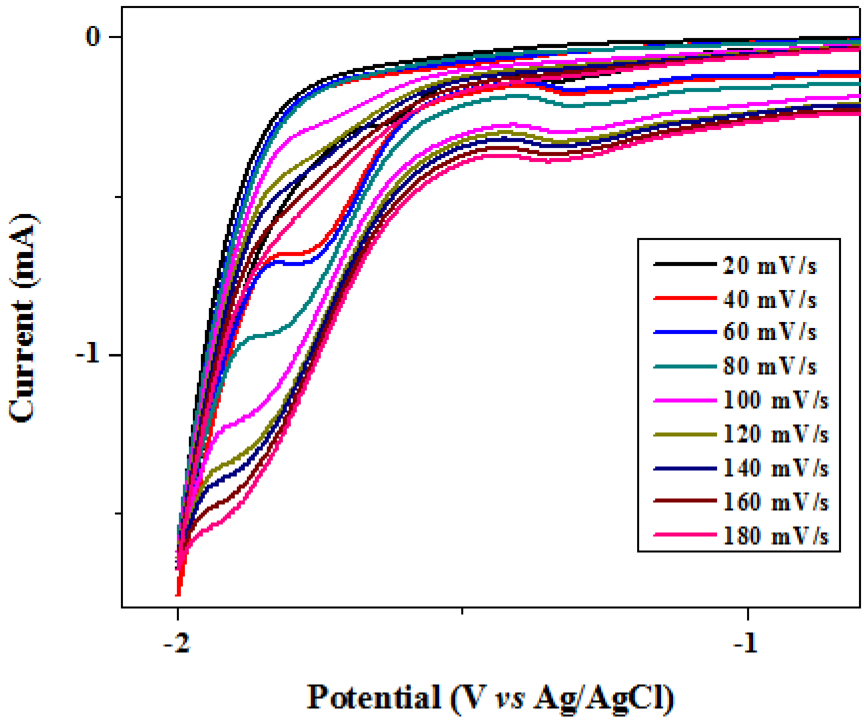

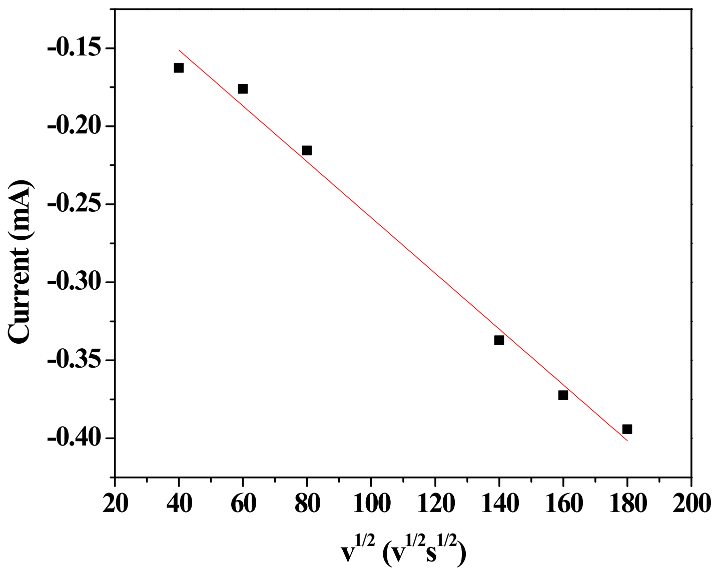

Fig. S6. Scan rate dependence of precatalytic waves for a 0.10 mM solution of complex **1** in buffer (pH 7.0), at scan rates from 20 to 180 mV/s.

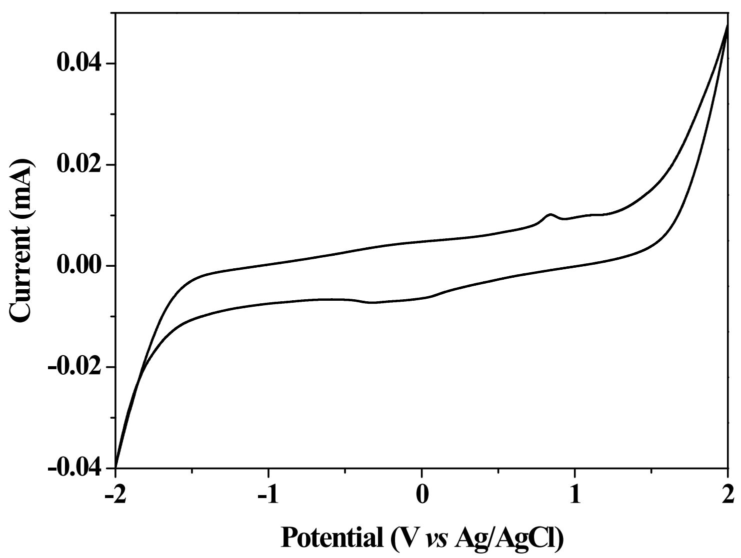

Fig. S7. Cyclic voltammogram of ligand (1.196 mM) in water and a scan rate of 100 mVs^{-1}.

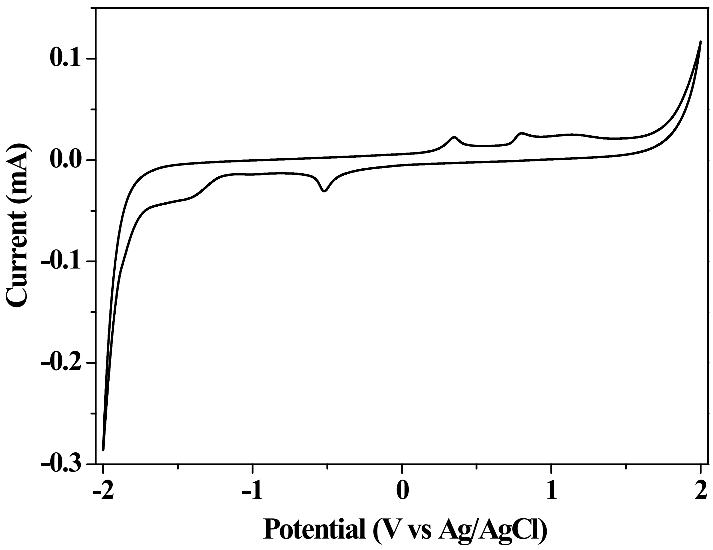

Fig. S8. Cyclic voltammogram of $CuSO_4$ (1.196 mM) in water and a scan rate of 100 mVs^{-1}.

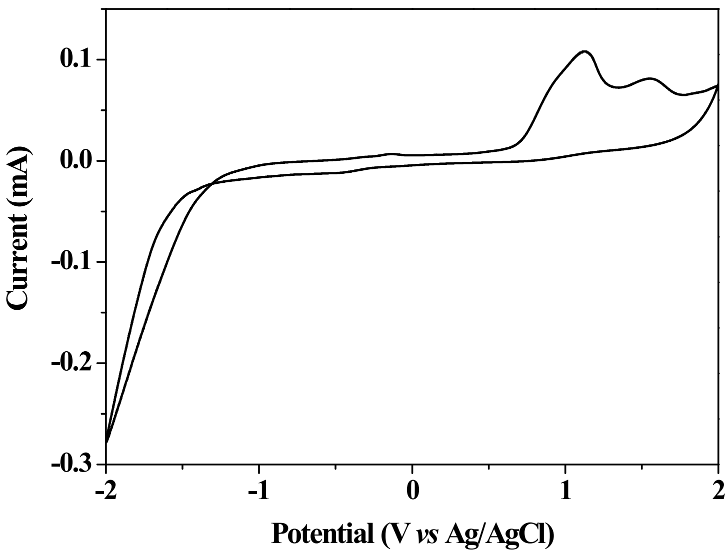

Fig. S9. Cyclic voltammogram of $CuSO_4$ (2.4 mM) and ligand (1.196 mM) in water and a scan rate of 100 mVs^{-1}.

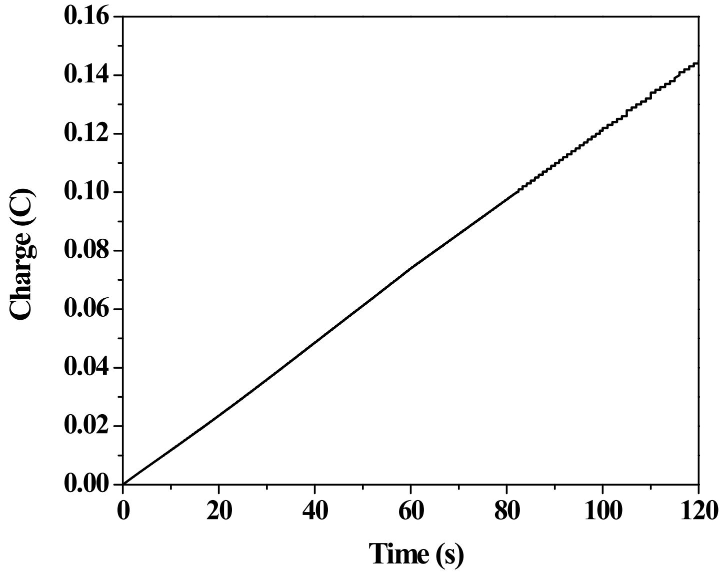

Fig. S10. Charge buildup versus time at -1.45 V *vs* Ag/AgCl in a 0.25 M phosphate buffer at pH 7.0.

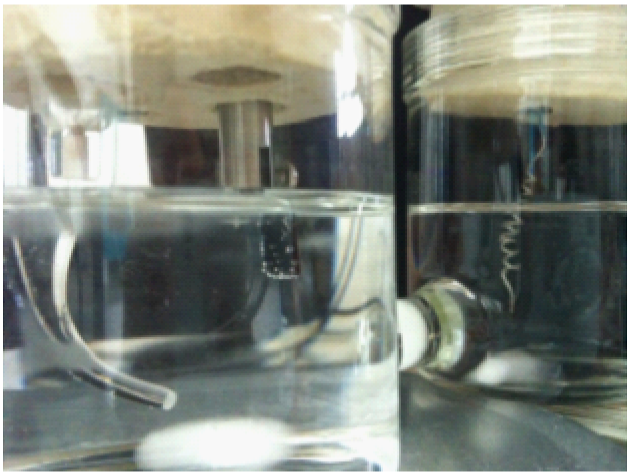

Fig. S11. H_2 bubbles

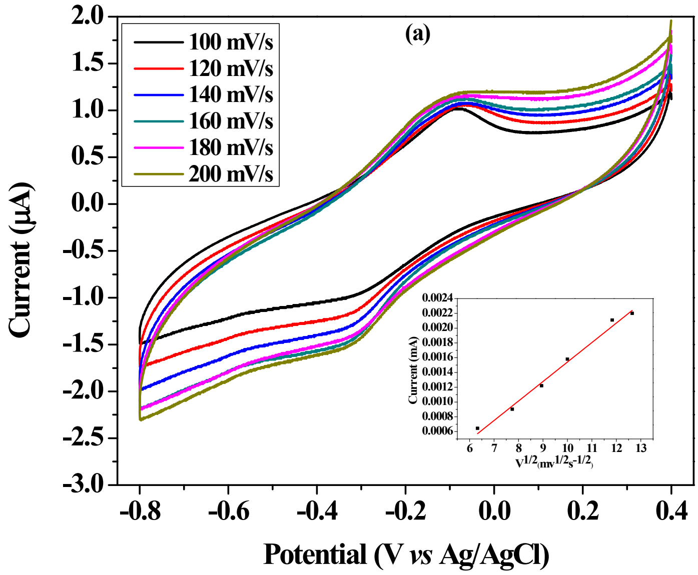
(a)
100 mV/s
120 mV/s
140 mV/s
160 mV/s
180 mV/s
200 mV/s
Current (μA)
Potential (V vs Ag/AgCl)
Current (mA)
V1/2(mv1/2s-1/2)

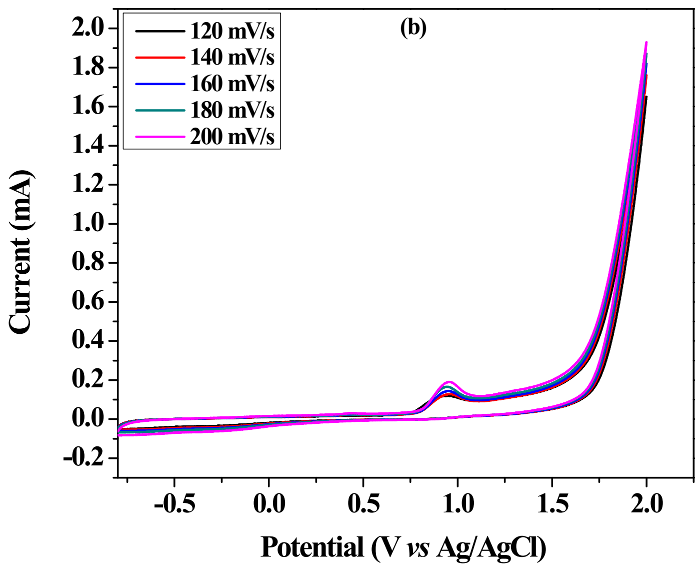
(b)
120 mV/s
140 mV/s
160 mV/s
180 mV/s
200 mV/s
Current (mA)
Potential (V vs Ag/AgCl)

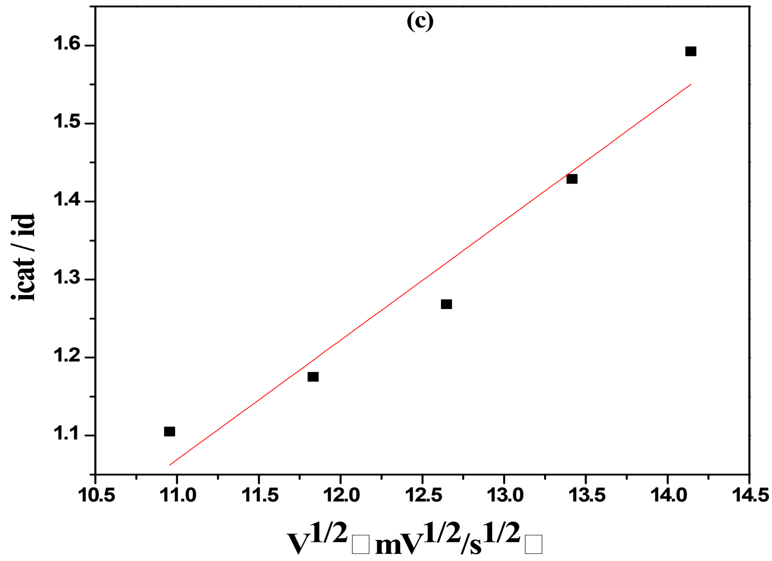

Fig. S12. (a) Dependence of the peak current for the $Cu^{II/I}$ couple at $E_{1/2}$= -0.21 V. (b) Scan rate dependence of precatalytic waves for a 0.10 mM solution of complex **1** in buffer (pH 8.7), at scan rates from 120 to 200 mV/s. (c) Linear fitting plot of i_{cat}/i_d *vs* $v^{-1/2}$ for TOF calculation.

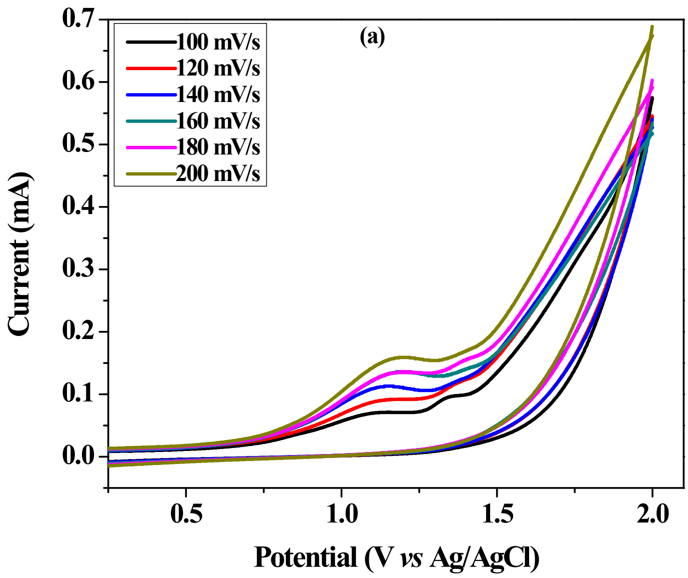

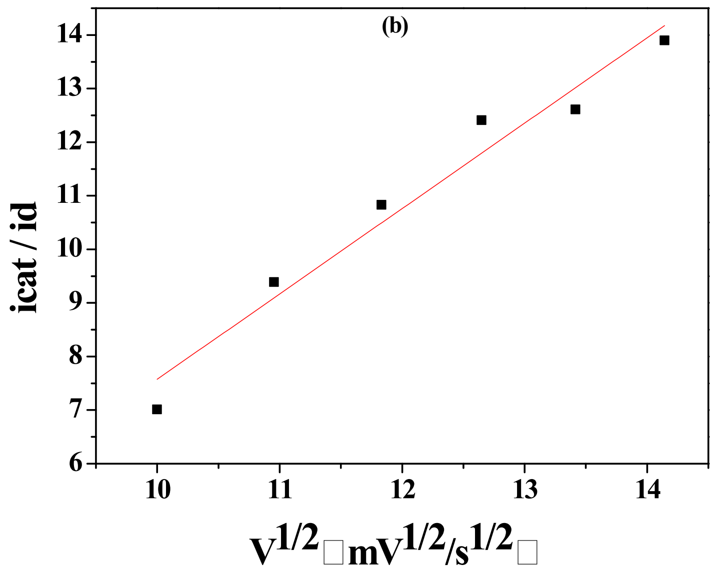

Fig. S13. (a) Scan rate dependence of precatalytic waves for the $Cu^{IV/III}$ couple at $E_{p,a}$ = 1.20 V in buffer (pH 10.8), at scan rates from 100 to 200 mV/s. (b) Linear fitting plot of i_{cat}/i_d *vs* $v^{-1/2}$ for TOF calculation.

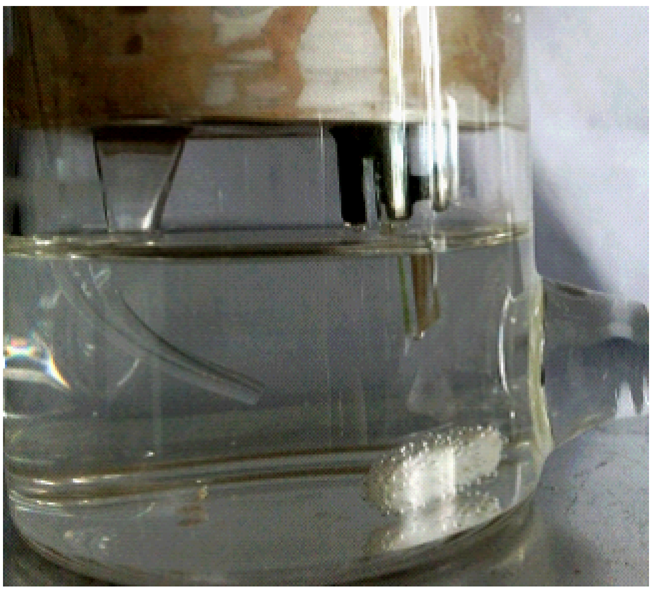

Fig. S14. O_2 bubbles

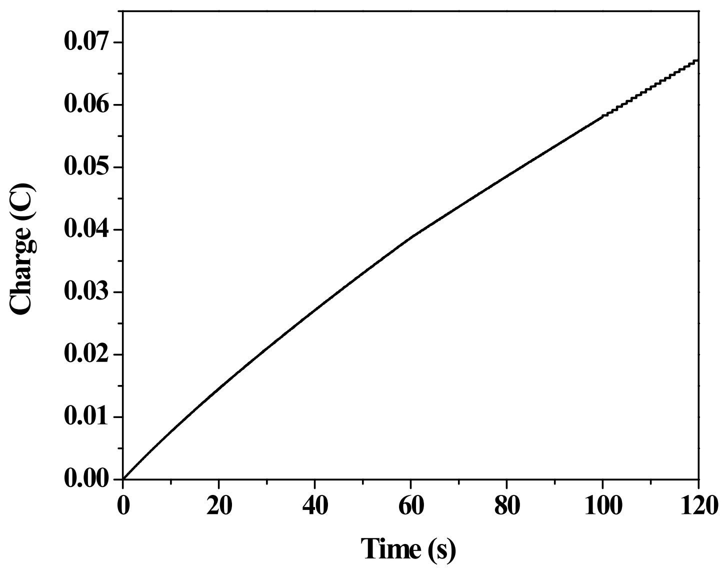

Fig. S15. Charge buildup of 0.25 M phosphate buffer at pH 10.8

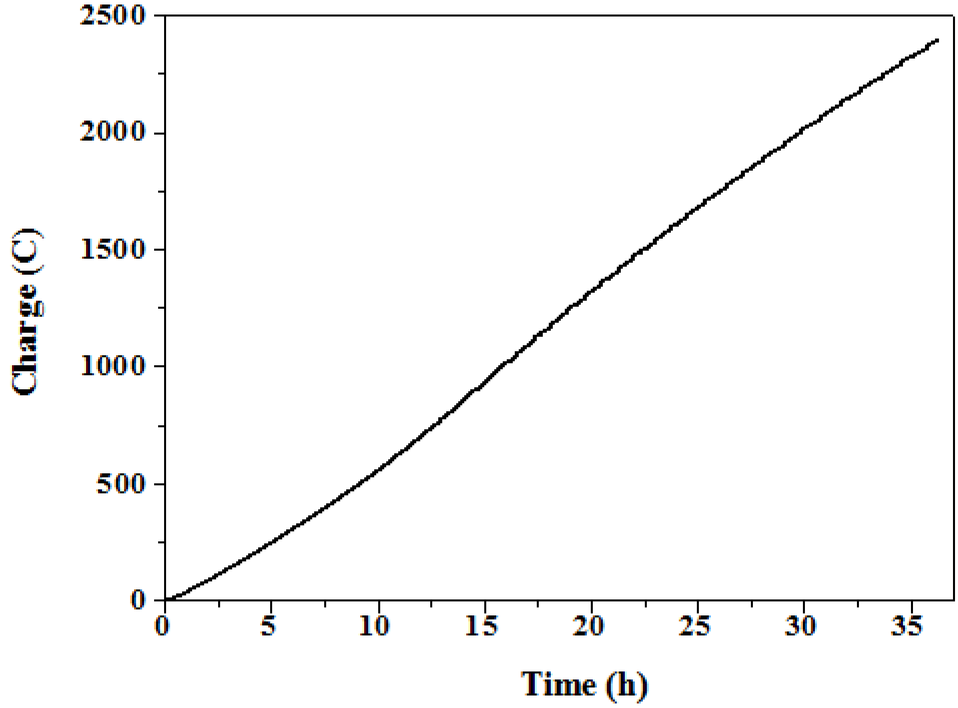

Fig. S16. Extended controlled potential electrolysis of 2.8 μM complex **1**, showing charge buildup versus time with an applied potential of -1.40 V *vs* Ag/AgCl Conditions: 0.25 M buffer solution, pH 7.0, GC working electrode (1.25 cm^2), Pt wire counter electrode, 36 h.

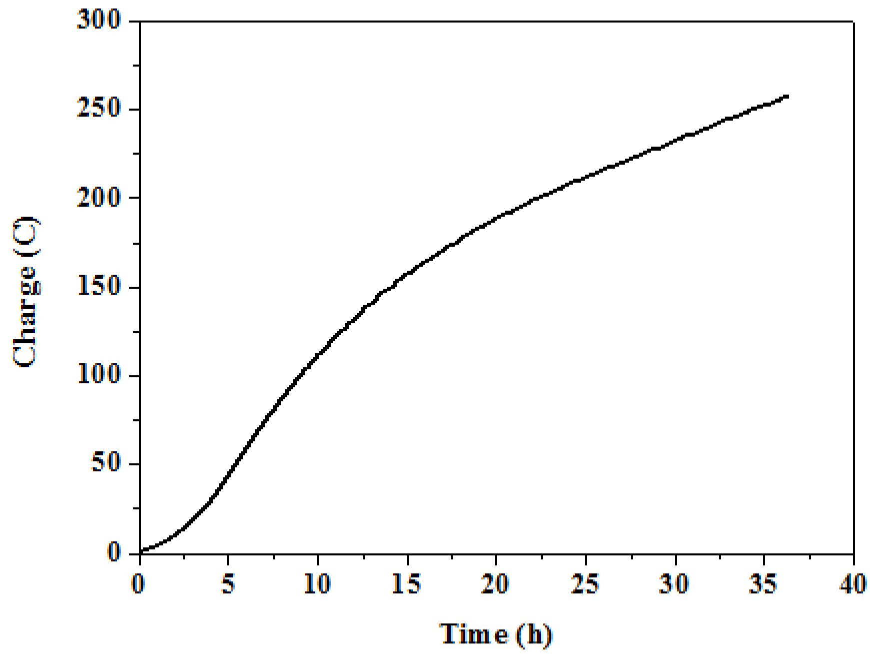

Fig. S17. Extended controlled potential electrolysis of 4.9 μM complex **1** in 0.25 M phosphate buffer at pH 10.8, showing charge buildup versus time with an applied potential of 1.40 V vs Ag/AgCl. ITO working electrode (1.25 cm^2), Pt counter electrode, 36 h.

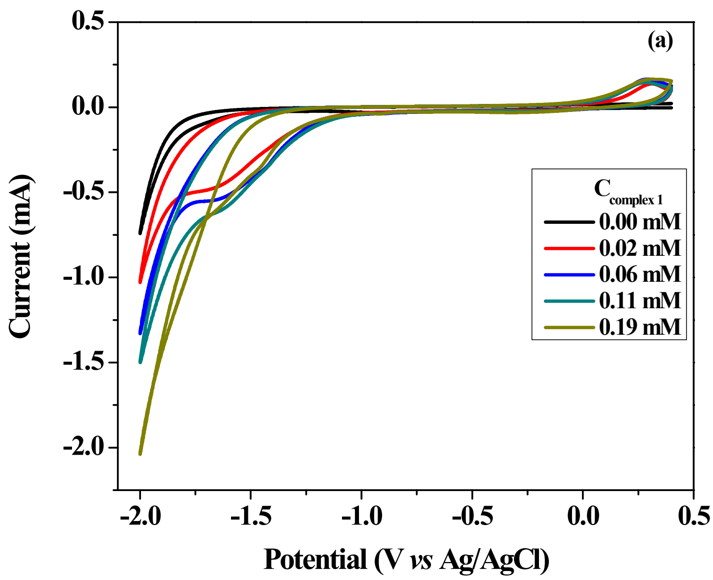

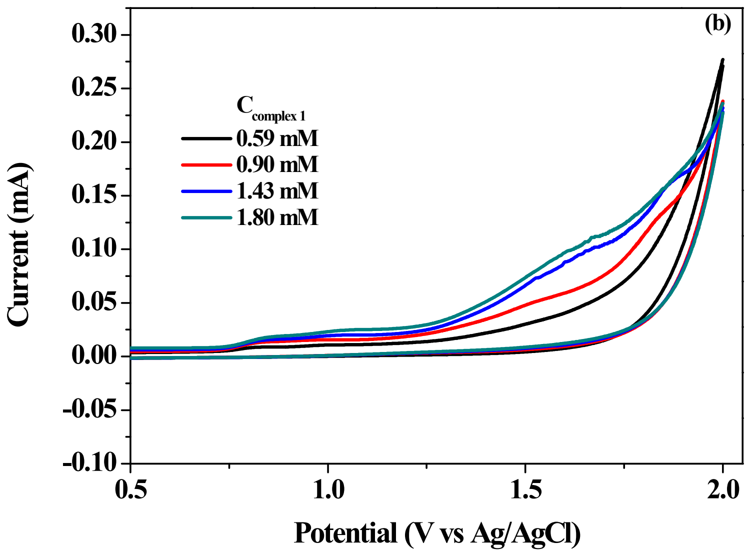

Fig. S18. (a) Cyclic voltammograms of complex **1** (0.10 mM) in 0.25 M phosphate buffer (pH 7.0) at a glassy carbon electrode and a scan rate of 100 mV/s with different concentration for (a) water reduction and (b) water oxidation.

$$\frac{i_c}{i_p} = 0.359\frac{n_c}{n_p^{3/2}}\sqrt{k_{cat}/\upsilon} \qquad (1)$$

y=-0.5278x-6.140

n=4; n_p= 1

$$\frac{i_c}{i_p} = 0.359\frac{n_c}{n_p^{3/2}}\sqrt{k_{cat}/\upsilon} = 1.413\sqrt{k_{cat}} \times \upsilon^{-1/2}$$

$$1.413\sqrt{k_{cat}} = -0.5278$$

$$k_{cat} = 0.14s^{-1}$$

Eq. 2 The calculation of TOF-1

$$\frac{i_c}{i_p} = 0.359\frac{n_c}{n_p^{3/2}}\sqrt{k_{cat}/\upsilon} \qquad (1)$$

y=1.593x-8.357

n=4; n_p= 1

$$\frac{i_c}{i_p} = 0.359\frac{n_c}{n_p^{3/2}}\sqrt{k_{cat}/\upsilon} = 1.413\sqrt{k_{cat}} \times \upsilon^{-1/2}$$

$$1.413\sqrt{k_{cat}} = 1.593$$

$$k_{cat} = 1.13s^{-1}$$

Eq. 3 The calculation of TOF-2